

# The Enlarged d-q Model of Induction Motor with the Iron Loss and Saturation Effect of Magnetizing and Leakage Inductance

Jan Otýpka, Petr Orság, Vítězslav Stýskala, Dmitrii Kolosov, Stanislav Kocman and Feodor Vainstein

**Abstract** The main aim of this paper is the presentation of induction motor model with the iron loss and the saturation effect of magnetizing and leakage inductances. The previous published standard models of induction motor using the d-q model actually neglect the iron loss effect. Hence, the iron loss represents about 3–5 % total loss in the induction motor. This paper is focused on the inferred model, which considers the iron loss in motor, and comparing with the standard models. The second part of the paper deals with the saturation effect of magnetizing and leakage inductances.

**Keywords** Induction motor · D-q coordinate frame model · Iron loss · Saturation effect · Magnetizing inductance · Leakage inductance · T-form

## 1 Introduction

The conventional model of induction motor is based on the classical T-form layout without the iron loss. This model is widely used for the operation of induction motor. The conventional model is presented many researchers [1–4]. In case of the operation of such motor with minimal losses or the power dynamic analysis of induction motors powered by the harmonic or nonharmonic source, the conven-

---

J. Otýpka · P. Orság · V. Stýskala · D. Kolosov (✉) · S. Kocman  
Department of Electrical Engineering FE ECS, VŠB—Technical University of Ostrava,  
17. Listopadu 15, 708 33 Ostrava, Poruba, Czech Republic  
e-mail: dmitrii.kolosov@vsb.cz

J. Otýpka  
e-mail: jan.otypka@vsb.cz

F. Vainstein  
STEM College, Texas A&M University Texarkana, 7101 University Ave, Texarkana,  
TX 75503, USA  
e-mail: Feodor.Vainstein@tamut.edu

tional model is not sufficient for the using. Hence, this model must be enlarged with the consideration of the iron loss.

This paper presents the enlarged model with the iron loss in d-q coordinate frame system. New model is compared with the conventional model for the starting of induction motor without a load. Each kind of loss is calculated by this model as the conventional model considers only the stator and rotor windings losses. On the other hand, the iron loss is not separated from the eddy-current loss and hysteresis loss, because the physical interpretation of both losses is relatively complicated. The possible solving of this problem is published in [5]. Therefore, the enlarged model operates only with one value of the resistance  $R_{Fe}$  represented the iron loss, which includes both losses.

This paper is also focused on the saturation effect of magnetizing and leakage inductances, which are considered to be constant according to the stator and rotor currents for the standard solving. These nonlinear parameters are obtained by the identification method from the short circuit test and the idle test, which were measured on the specific type of induction motor. The model involves the blocks for direct calculation of the actual values of saturated magnetizing inductance and stator and rotor leakage inductances, which are given by nonlinear dependence on the magnetizing, stator and rotor currents. The topic conclusion is devoted to the simulation results of induction motor starts with the linear and nonlinear models.

## 2 The Model of Induction Motor with Iron Loss

The conventional model of induction motor is based on the classical equivalent circuit in T-form, from which derives the d-q coordinate frame model, presented in [1–4]. If this model is enlarged by the additional iron loss resistance  $R_{Fe}$ , the currents flowing in the transversal branch must be defined. The transversal branch is presented by the parallel combination of iron loss resistance  $R_{Fe}$  and magnetizing inductance  $L_m$ . The model of induction motor with the considering of iron loss is obtained, when the model derivation is based on the magnetizing current  $i_m$ , which flows through the magnetizing inductance  $L_m$ .

The derivation of the induction motor model is obtained from Fig. 1, where the currents (the main current  $i_0$ , which flows through the transversal branch and the current in iron  $i_{Fe}$ ) are defined by using the current divider. These currents are obtained as the function of the magnetizing current  $i_m$ . This approach for derivation of the induction motor model with iron loss is presented in [3, 6, 7].

The model of induction motor with the iron loss is given by these equations presented in [3, 6, 7] for the general d-q coordinate frame system, which rotates with the general angle speed  $\omega$ :

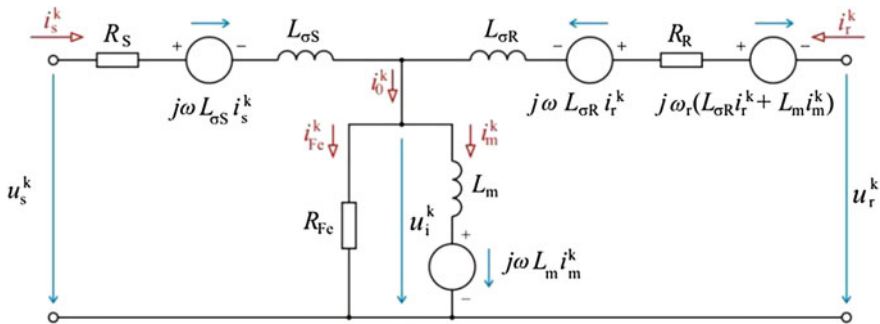


**Fig. 1** The equivalent circuit model of induction motor in T-form with the iron loss

$$u_{ds}^k = R_S i_{ds}^k + L_{\sigma S} \frac{di_{ds}^k}{dt} + L_m \frac{di_{dm}^k}{dt} - \omega (L_{\sigma S} i_{qs}^k + L_m i_{qm}^k), \quad (1)$$

$$u_{qs}^k = R_S i_{qs}^k + L_{\sigma S} \frac{di_{qs}^k}{dt} + L_m \frac{di_{qm}^k}{dt} + \omega (L_{\sigma S} i_{ds}^k + L_m i_{dm}^k), \quad (2)$$

$$u_{dr}^k = R_R i_{dr}^k + L_{\sigma R} \frac{di_{dr}^k}{dt} + L_m \frac{di_{dm}^k}{dt} - (\omega - \omega_r) (L_{\sigma R} i_{qr}^k + L_m i_{qm}^k), \quad (3)$$

$$u_{qr}^k = R_R i_{qr}^k + L_{\sigma R} \frac{di_{qr}^k}{dt} + L_m \frac{di_{qm}^k}{dt} + (\omega - \omega_r) (L_{\sigma R} i_{dr}^k + L_m i_{dm}^k), \quad (4)$$

$$i_{d0}^k = i_{ds}^k + i_{dr}^k, \quad (5)$$

$$i_{q0}^k = i_{qs}^k + i_{qr}^k, \quad (6)$$

$$i_{d0}^k = i_{dFe}^k + i_{dm}^k = i_{dm}^k + \frac{L_m}{R_{Fe}} \left( \frac{di_{dm}^k}{dt} - \omega i_{dm}^k \right), \quad (7)$$

$$i_{q0}^k = i_{qFe}^k + i_{qm}^k = i_{qm}^k + \frac{L_m}{R_{Fe}} \left( \frac{di_{qm}^k}{dt} + \omega i_{qm}^k \right), \quad (8)$$

where  $\omega_r$  is the electrical rotor angle frequency. The magnetic fluxes components are given by the equations in axis d and q:

$$\Psi_{ds}^k = L_{\sigma S} i_{ds}^k + L_m i_{dm}^k, \quad (9)$$

$$\Psi_{qs}^k = L_{\sigma S} i_{qs}^k + L_m i_{qm}^k, \quad (10)$$

$$\Psi_{dr}^k = L_{\sigma R} i_{dr}^k + L_m i_{dm}^k, \quad (11)$$

$$\Psi_{qr}^k = L_{\sigma R} i_{qr}^k + L_m i_{qm}^k. \quad (12)$$

The induced voltage on the magnetizing branch is defined by the following equations in d-q coordinate frame:

$$u_{di}^k = L_m \frac{di_{dm}^k}{dt} - \omega L_m i_{dm}^k, \quad (13)$$

$$u_{qi}^k = L_m \frac{di_{qm}^k}{dt} + \omega L_m i_{qm}^k. \quad (14)$$

The electromagnetic torque in general d-q coordinate frame is given by the interaction between rotor magnetic fluxes components and stator currents components:

$$T_{em} = \frac{3}{2} p_p \frac{L_m}{L_{\sigma R} + L_m} \left[ \Psi_{qr}^k (i_{ds}^k - i_{dFe}^k) - \Psi_{dr}^k (i_{qs}^k - i_{qFe}^k) \right], \quad (15)$$

The mechanical equation is given by:

$$J \frac{d\Omega_m}{dt} = T_{em} - T_L - k_F \Omega_m, \quad (16)$$

where  $\Omega_m$  is the mechanical angle speed,  $J$  is inertia,  $T_L$  is load torque and  $k_F$  is friction coefficient. The calculation of total losses is presented in [8], thereafter the total losses in model could be separated to dissipated power by the joule effect in stator and rotor winding and the iron loss. The total losses are given by:

$$\begin{aligned} \Delta P_{\text{celk.}} &= \Delta P_{j.s} + \Delta P_{j.r} + \Delta P_{Fe} \\ &= \frac{3}{2} \left[ R_S (i_{ds}^2 + i_{qs}^2) + R_R (i_{dr}^2 + i_{qr}^2) + \frac{1}{R_{Fe}} (u_{di}^2 + u_{qi}^2) \right]. \end{aligned} \quad (17)$$

The induction motor identified parameters are given in Table 1. The parameters of longitudinal branch: rotor resistance  $R_R$ , leakage inductances  $L_{\sigma S}$  a  $L_{\sigma R}$  are obtained from the short circuit test. The parameters of transversal branch: magnetizing inductance  $L_m$  and the iron loss resistance  $R_{Fe}$  are obtained from the idle test. These parameters are considered to be constant in simulation.

The model of induction motor with the iron loss is created in the Matlab Simulink environment. The simulation is focused on the starting process without load, when the enlarged model of induction motor with the iron loss is compared with the conventional model. Both models are simulated in stationary d-q frame for angle speed  $\omega = 0$  rad/s and supply voltage has amplitude 325 V with frequency 50 Hz. The simulation results are presented at Figs. 2, 3, 4, 5, 6 and 7, where the

**Table 1** The table of identified parameters for specific type of induction motor

Parameter	Sign	Value
Nominal power	$P_N$	4 kW
Nominal voltage	$U_N$	400 V
Nominal current	$I_N$	8.1 A
Nominal frequency of mains	$f_N$	50 Hz
Nominal speed	$n_n$	1440 rpm
Effectivity class		IE2
Stator resistance	$R_S$	1.1 $\Omega$
Stator leakage inductance	$L_{\sigma S}$	9.5 mH
Rotor resistance	$R_R$	1.478 $\Omega$
Rotor leakage inductance	$L_{\sigma R}$	14.8 mH
Magnetizing inductance	$L_m$	172.7 mH
Equivalent resistance for core loos	$R_{Fe}$	491 $\Omega$
Inertia	$J$	0.02 kg m <sup>2</sup>

**Fig. 2** The waveform of electromagnetic torque for both models

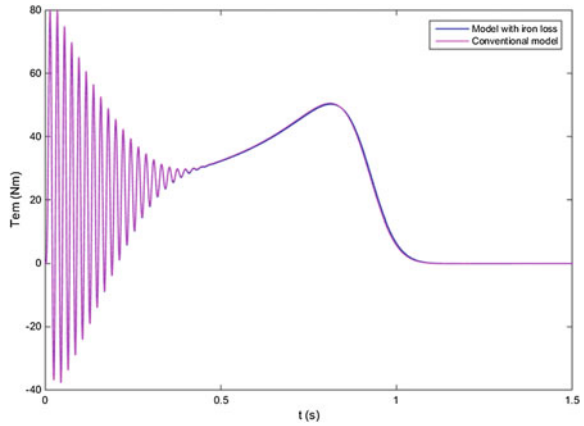


**Fig. 3** The waveform of stator current in first phase for both models

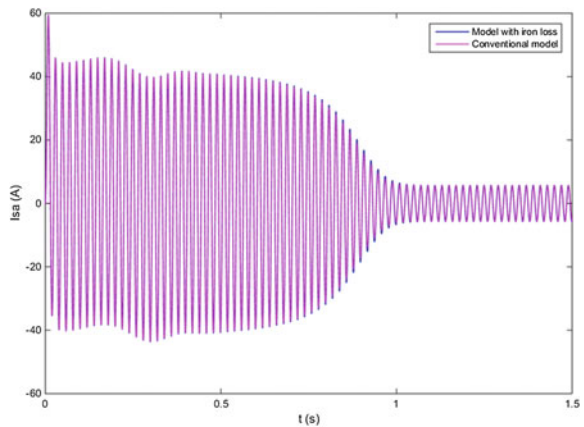


**Fig. 4** The detail of stator current waveform for both models

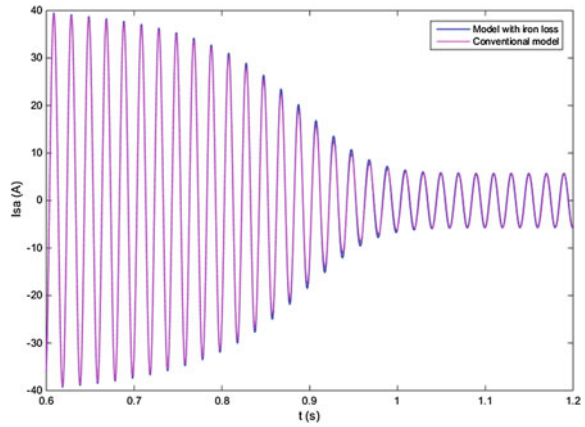


**Fig. 5** The absolute value of magnetizing current  $i_m$  given by the vector sum of components in d and q axis for enlarged model of induction motor

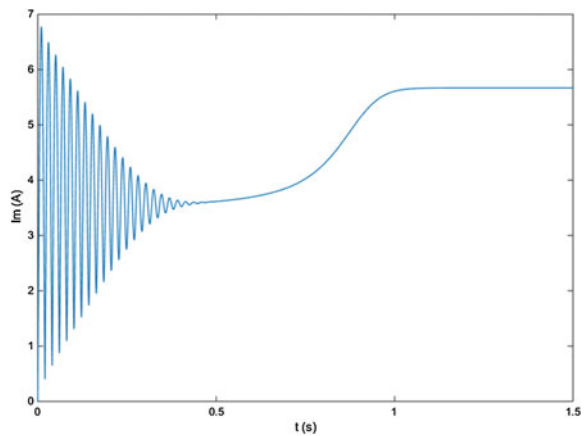


**Fig. 6** The absolute value of iron current  $i_{Fe}$  given by the vector sum of components in d and q axis for enlarged model of induction motor

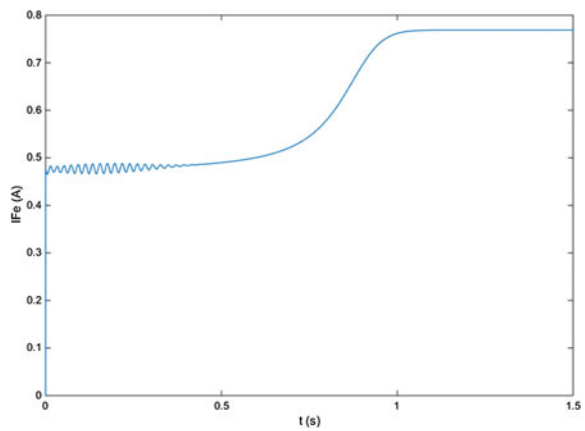
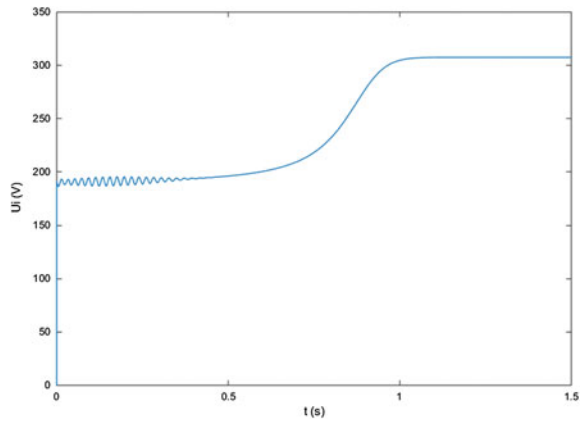


**Fig. 7** The absolute value of inducted voltage over magnetizing branch  $u_i$  given by the vector sum of components in d and q axis for enlarged model of induction motor



electromagnetic torque  $T_{em}$ , the stator current of first phase  $i_{sa}$ , the magnetizing current  $i_m$ , the iron current  $i_{Fe}$  inducted voltage over magnetizing branch  $u_i$  are shown.

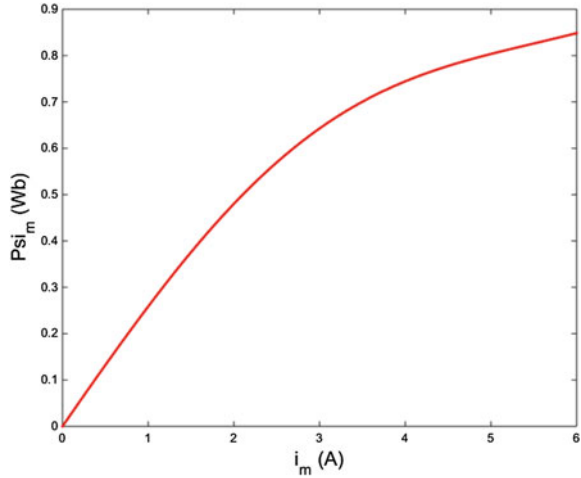
### 3 The Saturating Effect of Magnetizing and Leakage Inductance in Induction Motor

The parameters like magnetizing inductance, stator and rotor leakage inductance are considered to be constant in the previous simulations of induction motor. Therefore, the magnetizing flux and leakage fluxes are taken as the linear functions of magnetizing current or stator and rotor currents. In fact, the magnetizing inductance is saturated, thus the magnetizing flux is nonlinear versus the magnetizing current, as it is described in [9, 10] and it is shown on Fig. 8. The similar effect could be observed for the leakage fluxes, which pass predominantly through the air. Hence, the stator and rotor leakage fluxes are conventionally expected to be linear depending on the stator and rotor currents. However, a little part of the stator and rotor leakage fluxes passes through the iron, because the leakage inductances are nonlinear to the stator and rotor current. This issue is solved in [11–13].

#### 3.1 The Saturating Effect of Magnetizing Inductance

The main magnetizing flux is nonlinear to the magnetizing current of induction motor, as it is shown on Fig. 8. This fact is proved by the analysis from the idle test measured in the steady state. These nonlinear dependence of magnetizing flux  $\Psi_m$  and magnetizing current  $i_m$  can be approximated by the odd order polynomial function. The reason is that the supply voltage consists of the characteristic

**Fig. 8** The nonlinear dependence of magnetizing flux  $\Psi_m$  on magnetizing current  $i_m$



harmonic frequencies with general frequency  $f_1$  and only odd harmonic frequencies  $3f_1, 5f_1, 7f_1, \dots, pf_1$ , which are generated by the source and nonlinear magnetizing branch [10]. The nonlinear dependence between magnetizing flux and current can be approximated by the following function:

$$\Psi_m = k_1 i_m + k_3 i_m^3 + k_5 i_m^5 + k_7 i_m^7 + \dots, \quad (18)$$

where  $k_1, k_3, k_5$ , etc. are coefficients of polynomial function. The magnetizing inductance is defined by form:

$$L_{m,d} = \frac{d\Psi_m}{di_m}. \quad (19)$$

The nonlinear dependences of the magnetizing flux  $\Psi_m$  and the magnetizing inductance  $L_m$  on the magnetizing current  $i_m$ , which are obtained by the direct approximation from the measuring and parameters identification, these are shown on Figs. 8 and 9.

### 3.2 The Saturating Effect of Leakage Inductances

The nonlinear dependence is also determined for both leakage inductances  $L_{\sigma S}$  and  $L_{\sigma R}$ . This fact was verified from the short circuit test measured with reduced voltage. It is evident in Fig. 11 that the leakage inductances have higher values in the range of low currents comparing with the nominal current. This important fact must be included to the model of induction motor. This issue is described in [11–13].

**Fig. 9** The nonlinear dependence of magnetizing inductance  $L_m$  on magnetizing current  $i_m$

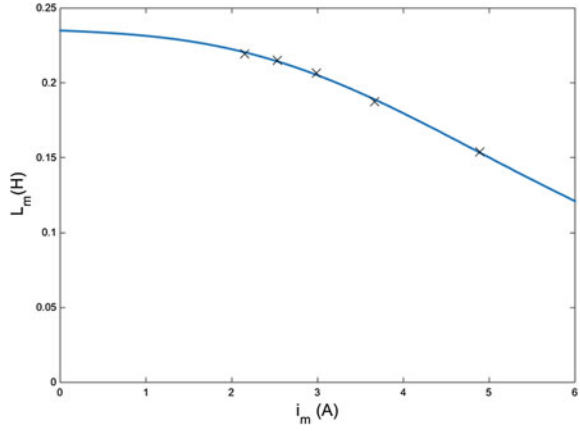


**Fig. 10** The nonlinear dependence of leakage fluxes on stator current

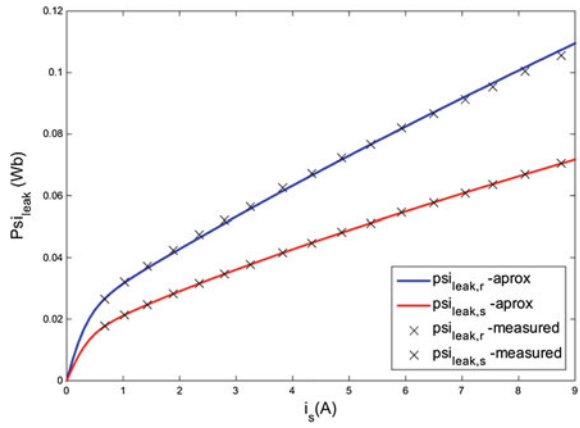
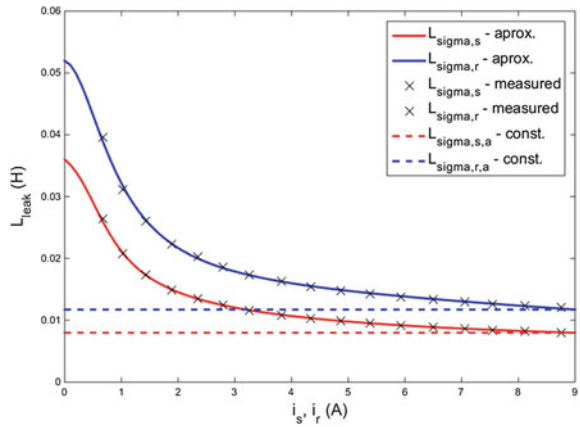


**Fig. 11** The nonlinear dependence of leakage inductances on stator and rotor current



The stator and rotor leakage inductance are separated into the constant components and nonlinear components according to [11, 12]. Thereafter, the leakage inductances are given by:

$$L_{\sigma S} = L_{\sigma S,a} + L_{\sigma S,i}(i_s), L_{\sigma R} = L_{\sigma R,a} + L_{\sigma R,i}(i_r), \quad (20)$$

where  $L_{\sigma S,a}$  and  $L_{\sigma R,a}$  are the linear components of leakage inductances in the air and  $L_{\sigma S,i}(i_s)$  and  $L_{\sigma R,i}(i_r)$  are nonlinear components of leakage inductances in the iron, which depend on the stator and rotor currents. The nonlinear dependences of the leakage fluxes and inductances on currents are shown on Figs. 10 and 11, which were obtained by the short circuit test.

### 3.3 Simulation Results

The model of induction motor with the iron loss according to Eqs. (1)–(17) was enlarged by the saturating effect of magnetizing inductance  $L_m$  and leakages inductances  $L_{\sigma S}$  and  $L_{\sigma R}$ . Each inductance is implemented by the polynomial function to the model, which calculates the values of inductances from the actual values of each current. The general schema is presented on Fig. 12.

The model with the iron loss and constant parameters is compared with the both models, which includes the saturation effect of magnetizing inductance and leakage inductances (model with only saturated magnetizing inductance and model with each saturated inductance). The simulation results are better illustrated by the electromagnetic torque waveform, see Fig. 13.

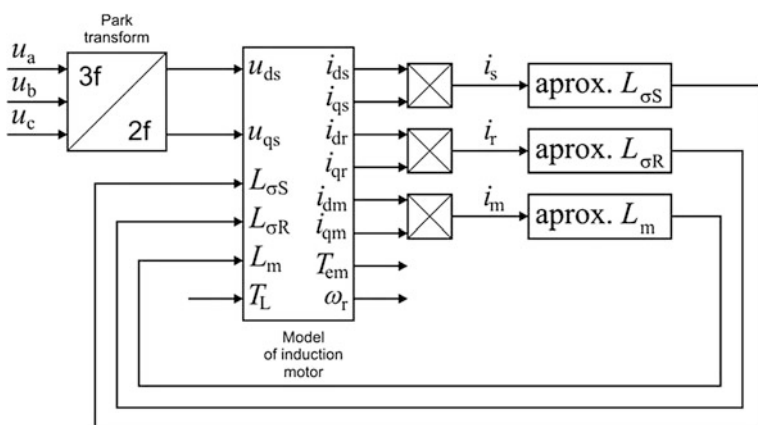
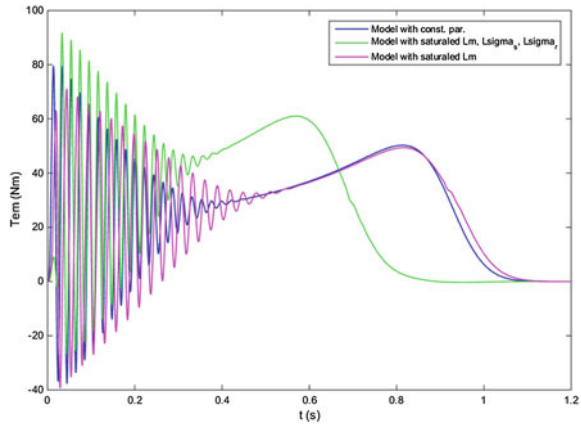


**Fig. 12** The model of induction motor with calculation of magnetizing, stator and rotor leakage inductance

**Fig. 13** The electromagnetic torque waveform simulated by introduced models



## 4 Conclusion

The simulation results show that the differences between the conventional model and the enlarged model with iron loss are negligible for normal operating conditions. The minor differences may appear in dynamic states. This fact is shown in Figs. 2, 3 and 4, where the starting process of induction motor is shown. The correct solution of model with iron loss is confirmed, as the iron current is much smaller than magnetizing current ( $i_{Fe} \ll i_m$ ). Therefore, the iron current does not considerably affect the stator current, as is shown in Figs. 3 and 4. The simulated iron current caused the power dissipation 350 W in the steady state, confirms the values measured during the idle test.

It is evident in Fig. 13, that the nonlinear dependence of inductances on currents have major impact for simulation of torque, motor currents and speed waveforms, because the electrical time constant is dynamically changed due to the inductance calculations. The saturating effect has the major impact on the dynamic changes in the models of induction motor against the model with constant parameters.

**Acknowledgments** The work is partially supported by Grant of SGS No. SP2015/151, VŠB—Technical University of Ostrava, Czech Republic.

## References

1. Krause, P.C., Wasynczuk, O., Sudhoff, S.D.: Analysis of Electric Machinery and Drive Systems. IEEE Press, NY (2002)
2. Leedy, A.W.: Simulink/MATLAB Dynamic Induction Motor Model for use in Undergraduate Electric Machines and Power Electronics Courses. IEEE, NY (2013)
3. Neborák, I.: Modelování a simulace elektrických regulovaných pohonů. Monografie, VŠB-TU Ostrava 2002, 172 stran, ISBN 80-248-0083-7

4. Giri, F.: *AC Electric Motors Control: Advanced Design Techniques and Applications*. Wiley (2013) ISBN 978-1-118-33152-1
5. Kioskeridis, I., Margaritis, N.: Loss minimization in induction motor adjustable-speed drives. *IEEE Trans. Ind. Electron.* **43**, 226–231 (1996)
6. Jung, J.: A vector control scheme for EV induction motors with a series iron loss model. *IEEE Trans. Ind. Electron.* **45**, 617–624 (1998)
7. Moulahoum, S., Touhami, O.: *A Saturated Induction Machine Model with Series Iron Losses Resistance*. IEEE, Power Engineering, Energy and Electrical Drives (2007)
8. Lim, S., Nam, K.: Loss-minimising control scheme for induction motors. *IEE Proc. Electr. Power Appl.* **151**, 385–397 (2004)
9. Levi, E.: A unified approach to main flux saturation modeling in D-Q axis models of induction machines. *IEEE* **10**, 455–461 (1995)
10. Kerkman, R.J.: Steady-state and transient analysis of an induction machine with saturation of the magnetizing branch. *IEEE Trans. Ind. Appl.* **21**(1), 226–234 (1985)
11. Lipo, T.A., Consoli, A.: Modeling and simulation of induction motors with saturable leakage reactances. *IEEE Trans. Ind. Appl.* **IA-20**(1), 180–189 (1981)
12. Keyhani, A., Tsai, H.: IGSPICE simulation of induction machines with saturation inductance. *IEEE Trans. Energy Convers.* **4**(1) (1989)
13. Alsammak, A.N.B., Thanoon, M.F.: An improved transient model of an induction motor including magnetizing and leakage inductances saturated effect. *Int. J. Eng. Innovative Technol.* **3**(10) (2014)



<http://www.springer.com/978-3-319-27642-7>

Intelligent Systems for Computer Modelling  
Proceedings of the 1st European-Middle Asian  
Conference on Computer Modelling 2015, EMACOM  
2015

Stýskala, V.; Kolosov, D.; Snášel, V.; Karakeyev, T.;  
Abraham, A. (Eds.)

2016, XIII, 246 p. 130 illus., 39 illus. in color., Softcover  
ISBN: 978-3-319-27642-7